

Submitted to 32nd Lunar and Planetary Science Conference, March 12-16, 2001, Houston, Texas, Abstract 1927.

OXIDIZED AND HYDRATED SILICATES ON M- AND S- ASTEROIDS: SPECTRAL INDICATIONS.

V. V. Busarev, Sternberg State Astronomical Institute, Moscow University, Moscow, Russian Federation; e-mail: busarev@sai.msu.ru.

Introduction: It is generally supposed that M- and S- asteroids are remnants of differentiated parent bodies. This follows from their overall albedo and spectral characteristics corresponding to those of metal iron and igneous silicate assemblages [e. g., 1, 2]. But observational data suggesting the presence of oxidized or even hydrated silicates on the surfaces of the bodies were recently obtained [3-6]. In particular, it was shown that a considerable fraction (ab. 35%) of the main-belt M-type asteroids have absorption bands at 3 μm [3, 6] diagnostic of water of hydration. At the same time it was found that the visible-range reflectance spectra of some M- and S-asteroids include absorption features characterizing presence of oxidized silicates [4, 5]. Because of possible unusual combination of very different materials on the M- and S- asteroids the data should be correctly explained.

Results: On nights 17/18 and 18/19 September 1998 we obtained the visible and near-infrared spectra of two M-asteroids, 161 Athor (at phase angles of ab. 6.1° and 5.6°, respectively) and 497 Iva (phase angle ab. 6.8°) and of the C-asteroid 804 Hispania (phase

angle 3.5°). Spectra of the S- asteroid 198 Ampella were registered on 17/18 August 1999 (at phase angle 15.8°). The visible-range spectrum of the M-asteroid 21 Lutetia was measured on night 31 August/ 1 September 2000. For the purpose a CCD-spectrograph mounted on the 0.6 m telescope in the Crimea was used; a standard method for the reduction of the data was applied. At the same time the solar analog star, HD10307, was observed for subsequent calculation of the approximate asteroid reflectance spectra.

The reflectance spectra of 161 Athor (Fig. 1), 497 Iva (Fig. 2), 804 Hispania (Fig. 1 and 2), and 198 Ampella (Fig. 3) are combinations of “blue” (ab. 0.40-0.63 μm) and “red” (ab. 0.63-0.90 μm) parts observed separately at an interval of nearly two-minute. The initial reflectance spectra with a resolution of about 8 $\text{\AA}/\text{pix}$ were smoothed with a 40- \AA running box average and scaled to equal 1 at .55 μm . Some of the spectra in Fig. 1-3 are shifted up or down for clarity. Relative statistical errors in the spectra do not exceed 1-2% within the 0.45-0.80 μm wavelength range and grow up to 8% and

3% at “blue” and “red” ends, respectively. The reflectance spectrum of 201 Penelope with spectral resolution of about 50Å from [4] is given in Fig. 3 for comparison.

Discussion: As it was shown in [6], the M-asteroids 161 Athor and 497 Iva do not have absorption bands at 3 μm. Nevertheless, there are spectral indications of the presence of oxidized and probably hydrated silicates on their surfaces. We have reported before [5] that the reflectance spectrum of 161 Athor on 09/18/98 (Fig. 1) is typical for that of an M-asteroid, but another one on 09/17/98 corresponding to the opposite side of the body is similar to spectrum of the C-asteroid 804 Hispania. This part of the spectra of 161 Athor and of 804 Hispania in the range 0.40-0.50 μm exhibits a sharp drop at wavelengths shorter than 0.50 μm. It arises probably due to a strong ferric oxide intervalence charge transfer (IVCT) transition. There is a weak absorption band at 0.43 μm typical of ferric iron oxides [7] in the range too. Interestingly, the reflectance spectrum of 497 Iva (Fig. 2) turned out to resemble to the same reflectance spectrum of 804 Hispania in the range 0.68-0.98 μm. The range spans a wide absorption band probably connected with oxidized and hydrated silicates. Similar absorption features were found in reflectance spectra of primitive (C-, P-, D-, F-, and G-type) asteroids [8, 9]. The bands are generally attributed to iron oxides in phyllosilicates formed

on the asteroid surfaces by aqueous alteration processes. Such an interpretation is based upon known spectral characteristics of possible analogs of the asteroids among carbonaceous chondritic meteorites of types 1 and 2 (e. g., Nogoya and Mighei). The meteorites are assumed to be the result of the melting of ice and subsequent aqueous alteration of rocky materials in their parent bodies [10]. The process might have took place also in external shells of parent bodies of M- and S-asteroids.

Similar absorption features are also present in the visible-range reflectance spectra of the M-asteroids 201 Penelope and 21 Lutetia having absorption bands at 3 μm (according to [6]) and in reflectance spectrum of the S-asteroid 198 Ampella (Fig. 3).

We suppose that majority of the bands are superposition of absorption features of a few mineral assemblages. The obtained spectral characteristics of the M- and S-asteroids are in agreement with overall characteristics of such rockforming minerals as pyroxenes, olivines and possibly their oxidized and hydrated products. For example goethites, chlorites, etc. may be the products. As is known from Earth's mineralogy, the minerals are widespread in nature and formed from pyroxenes, olivines and other iron-bearing minerals under weathering [11]. The wavelength positions of the features and interpretation of corresponding electronic mechanisms

(crystal field (CF) or IVCT transitions) are (according to [12, 13]): at UV-.50 μm (IVCT $\text{O}^{2-} \rightarrow \text{Fe}^{3+}$), .425-.430 μm (Fe^{2+} ; CF ${}^5\text{T}_2({}^5\text{D}) \rightarrow {}^3\text{T}_1({}^3\text{P})$), .435-.450 μm (Fe^{3+} ; CF ${}^6\text{A}_1({}^6\text{S}) \rightarrow {}^4\text{A}_1, {}^4\text{E}({}^4\text{G})$) and/or IVCT $\text{Fe}^{2+} \rightarrow \text{Fe}^{3+}$), .51-.53 (CF $\text{Fe}^{2+}, {}^5\text{T}_2({}^5\text{D}) \rightarrow {}^3\text{T}_2({}^3\text{F})$ and/or ${}^3\text{T}_1({}^3\text{H})$), .59-.72 μm (IVCT $\text{Fe}^{2+} \rightarrow \text{Fe}^{3+}$), .63 μm (IVCT $\text{Fe}^{2+} \rightarrow \text{Fe}^{3+}$), .75-.80 μm (CF ${}^6\text{A}_1 \rightarrow {}^4\text{T}_1({}^4\text{G})$), .85-.92 μm (CF ${}^5\text{T}_2({}^5\text{D}) \rightarrow {}^5\text{E}({}^5\text{D})$).

Conclusions: From the observational data we suppose that oxidized silicates may be widespread on the main-belt asteroids including differentiated bodies. Moreover, presence of a small amount of hydrated silicates survived during the collisional evolution in the asteroid belt is possible on the asteroids. The inference seems to be quite natural if we keep a wide view of the evolutionary history of the bodies. One should take into account the possibility of delivering oxidized and hydrated silicates to differentiated asteroids (or to their parent bodies) by icy planetesimals from the zones of accumulation of Jupiter and other giant planets [5]. The very mechanism was proposed to explain the origin of Earth's hydrosphere, atmosphere and biosphere [14].

References: [1] Gaffey M. J. (1986) *Icarus* 66, 468-486. [2] Bell J. F. et al. (1989). In *Asteroids II* (R. P. Binzel et al., Eds), 921-945, Univ. of Arizona Press, Tucson. [3] Rivkin A. S. et al. (1995) *Icarus* 117, 90-100. [4] Busarev

V. V. (1998) *Icarus* 131, 32-40. [5] Busarev V. V. (2000) *LPS XXXI*, abstract 1428. [6] Rivkin A. S. et al. (2000) *Icarus* 145, 351-368. [7] Sherman D. M. (1984) *Phys. Chem. Miner.* 12, 161-175. [8] Vilas F. and M. J. Gaffey (1989) *Science* 246, 790-792. [9] Vilas F. et al. (1993) *Icarus* 102, 225-231. [10] Tomeoka K. and P. Buseck (1985) *Geochim. Cosmochim. Acta* 49, 2149. [11] Winchell, A. N. (1949), *Optical Mineralogy*, In. Lit. Press, Moscow, 416-417 [in Russian]. [12] Khomenko V. M. and A. N. Platonov (1987) *Rockforming pyroxenes: optical spectra, colouring and pleochroism*. Naukova Dumka Press, Kiev, [in Russian]. [13] Bakhtin A. I. and B. S. Gorobets (1992) *Optical spectroscopy of minerals and ores and its application in geological prospecting work*. Kazan' Univ. Press, Kazan', [in Russian]. [14] Delsemme A. H. (2000) *Icarus* 146, 313-325.

Fig. 1:

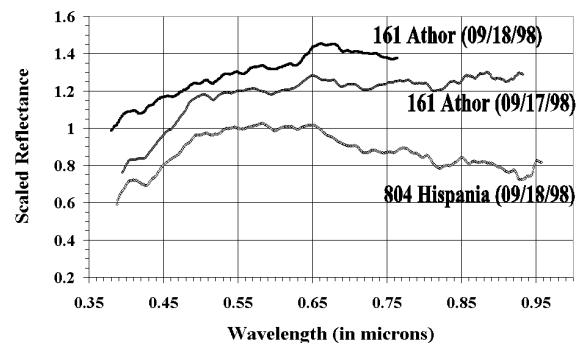


Fig. 2:

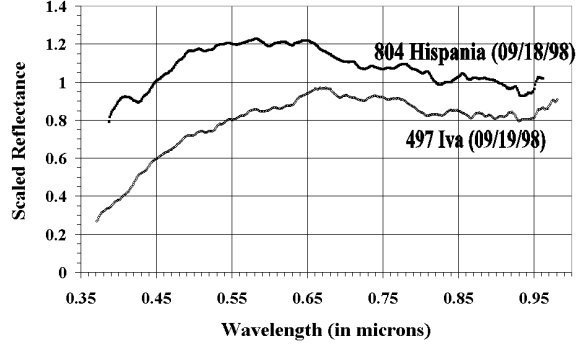


Fig. 3:

